Cover Page

Universiteit Leiden

The handle http://hdl.handle.net/1887/20094 holds various files of this Leiden University dissertation.

Author: Melis, Joost
Title: Nucleotide excision repair in aging and cancer
Date: 2012-11-06

Chapter 6

Chapter 6

Genotoxic exposure: novel cause of selection for a functional ΔN-p53 isoform

Melis JPM, Hoogervorst EM, van Oostrom CTM, Zwart E, Breit TM, Pennings JLA, de Vries A, van Steeg H.

Genotoxic exposure: novel cause of selection for a functional ΔN-p53 isoform

Oncogene. **2011** Apr 14;30 (15):1764-72.

"*But there's a warnin' sign, on the road ahead*"

Rockin' In The Free World – Neil Young, 1989

Abstract

The *p53* gene is frequently mutated in cancers and it is vital for cell cycle control, homeostasis and carcinogenesis. We describe a novel *p53* mutational spectrum, different to those generally observed in human and murine tumors. Our study shows a high prevalence of nonsense mutations in the p53 N-terminus of 2-AAF induced urinary bladder tumors. These nonsense mutations forced downstream translation initiation at codon 41 of *Trp53*, resulting in the aberrant expression of the p53 isoform ΔN-p53 (or p44). We propose a novel mechanism for the origination and the selection for this isoform. We show that chemical exposure can act as a novel cause of selection for this truncated protein. Additionally, our data suggest that the occurrence of ΔN-p53 accounts, at least in mice, for a cancer phenotype. We also show that gene-expression profiles of ES cells carrying the ΔN-p53 isoform in a p53 null background are divergent from p53 knock-out ES cells, and therefore postulate that ΔN-p53 itself has functional transcriptional properties.

Introduction

The tumor suppressor p53 regulates significant cellular functions to prevent the initiation and prolongation of cancer and is intensively studied. Several isoforms of p53 have been identified [1-4] and point mutations influencing the functionality of p53 were elucidated and mimicked *in vivo* [5-9]. The p53 gene is the most frequently mutated gene in cancer and analysis of many different human tumor types have shown a high prevalence of missense mutations located primarily in the central DNA binding domain [10]. Frequently, these mutations result in the expression of mutant p53 proteins, which are often more stable than wild type p53 [11]. A small variety of isoforms, which lack an N-terminal and/or C-terminal part of the protein have been discovered [1;3] and can result in a dominant-negative inhibition of the wild type p53 protein [8]. Although, a gain-of-function phenotype of mutant p53 which enhances the oncogenic properties of p53 has also been proposed [12;13].

To gain more functional insight into p53 and the effect of alterations in its gene, several transgenic mouse models have been generated [14]. For example, the *Trp53*$^{+/-}$ model appears to be more susceptible than wild type mice to carcinogenesis, both spontaneous and chemically-induced [15;16]. We have previously investigated the effect of p53 heterozygosity to the exposure of the carcinogen 2-acetylaminofluorene (2-AAF), a strong inducer of urinary bladder tumors [16]. Since stress signals like DNA damage can affect p53 function, we also investigated *Trp53*$^{+/-}$ in combination with a deficiency in the DNA repair gene *Xpa.* Carcinogenesis in both models is putatively caused by *Trp53* mutations in the remaining wild type allele, demonstrated by the presence of mutated p53 protein in early atypical preneoplastic lesions and tumors [16]. Here, we reveal a mutational spectrum in tumors divergent from that generally observed after carcinogen exposure (http://p53.free.fr/index.html). A high frequency of predominantly N-terminal nonsense mutations was found in the *Trp53* gene resulting in the selective expression of an N-terminally truncated P53-isoform (ΔN-p53). We further investigated the impact of this isoform by creating and analyzing embryonic stem cells harboring a nonsense mutation at codon 5, expressing the ΔN-p53 isoform. We showed this isoform has functional transcriptional properties that differ from both wild type and p53 knock out cells.

Material and Methods

Induction of urinary bladder tumors

2-AAF induced urinary bladder tumors in *Trp53*$^{+/-}$ and *Xpa*$^{-/-}$*/Trp53*$^{+/-}$ mice were obtained from our previously reported study [16]. Briefly, mice were treated for 39 weeks with 300 ppm 2-AAF in the diet. Liver, spleen and urinary bladder were collected at autopsy and fixed in 3.8% formaldehyde. The formaldehyde fixed samples were embedded in paraffin wax, cut into 5 µm sections, and stained with haematoxylin and eosin (H&E).

Immunohistochemical detection of p53 protein

P53 protein accumulation was detected in paraffin embedded, formalin-fixed sections from urinary bladder tumors. Polyclonal CM5 antibody, which recognizes several epitopes of both wild type and mutant mouse p53 protein (Novacastra), the Pab240 antibody specific for mutant p53 protein (Labvision), and the 1C12 antibody (Cell Signaling) recognizing the N-terminal part of the p53 protein,

were used (previously described by Hoogervorst *et al., 2004*). The level of CM5, Pab240 and 1C12 staining was scored by dividing the area of p53 positive fields by the total area of the tumor * 100% and the final result was scored either negative (-; ≤ 5%) or positive (+; ≥ 5 %).

Trp53 *mutation analyses by DNA and cDNA sequencing*

Formalin fixed, paraffin embedded urinary bladder tumors were analyzed for *Trp53* mutations by direct sequencing of genomic DNA. P53 positive and negative fields were marked on the p53 stained slides. Tumor regions were isolated on an adjacent 14 µm section slides. Genomic DNA was isolated with the QIAamp DNA minikit (QIAgen) according to the manufacturer's protocol. The coding region of the *Trp53* gene, spanning from exon 2 to 8 was amplified using the HotStarTaq Master Mix Kit (QIAgen) and a dedicated set of primers (Supplemental figure 2, primer set 1). Subsequently, exon 2, exon 3 and 4, exon 5 and 6 plus exon 7 and 8 were reamplified by using primer set 2 (Supplemental figure 2).

Frozen bladder tumor sections were analyzed for *Trp53* mutations by RT-PCR. RNA was isolated with TRIzol reagent (Invitrogen) as described by the manufacturer's protocol. For RT-PCR, performed with the Titan One Tube RT-PCR System (Roche), the primers used are depicted in supplemental figure 2, primer set 3. Subsequently, exon 2 to 5, exon 5 and 6, exon 7 and 8 and exon 9 to 11 were reamplified by using the primers of primer set 4 (Supplemental figure 2).

Purified PCR products (QIAquick PCR Purification Kit, QIAgen) were directly sequenced using the Big Dye Terminator Sequence kit version 3.1 (Applied Biosystems) and an ABI 3700 DNA sequencer, with identical primers as used for reamplification PCR.

Generation of mutant embryonic stem (ES) cells

p53.E5stop and p53.E5stop.M41I mutant targeting vectors

The p53.E5stop and p53.E5stop.M41I targeting vectors were constructed by introducing single base pair mutations in exon 2 and/or exon 4 in a genomic p53 fragment (Figure 3 + supplemental figure 1). The mutations lead to a glutamic acid-to-stop and a methionine-to-isoleucine substitution at codon 5 and 41, respectively. Primer set 5 was used to introduce the mutations into the *Trp53* sequence (supplemental figure 2).

The targeting vectors (Figure 3 + supplemental figure 1) were constructed by cloning the mutated fragment into flanking genomic p53 fragments comprising intron 4 to 3' end of the gene [6] together with the transcriptional stop-cassette described by Olive et al [35]. This stop-cassette contains a puromycin selection marker flanked by LoxP-sites. Targeting vectors contained a pGK-DTA selection marker (kindly provided by F. Gertler, Massachusetts Institute of Technology) at the 3' end of the vector for negative selection.

Homologous-recombination experiments in ES cells

The targeting vectors (Figure 3 + supplemental figure 1) were linearized and electroporated into $p53^{-/-}$ D3 ES cells (kindly provided by prof. T. Jacks, MIT, Cambridge) using standard procedures [36]. Puromycin resistant ES cell clones were analyzed for correct homologous integration of the targeting vector by Southern blot analysis (Supplemental figure 1). Recombination was examined by using an exon 1 probe (previously described in Jacks et al., 1994) (EcoR1-Stu1 digestion) and a 1.3 kb probe spanning exons 7 to 9 (BamH1 digestion). Correctly targeted ES cell clones were expanded and electroporated with circular pMC-CreN plasmid (kindly provided by F. Alt, Harvard Medical School, Boston). Clones that had lost the selectable marker cassette were selected for, by adding puromycin to the culture medium. Correctly targeted clones that were used for blastocyst injection procedures or cellular assays were analyzed for additional (undesired) mutations.

Western blot analyses

Protein analyses were executed as previously described [37]. Western blotting was performed with CM5 anti-p53 rabbit polyclonal antibody (Novacastra). Primary antibodies were detected by incubating with HRP-linked donkey anti-rabbit IgG (Amersham Pharmacia Biotech) and staining was done using ECL-plus reagent (Amersham Pharmacia Biotech). Actin protein levels, detected by a peroxidase (HRP) linked anti-actin affinity purified goat polyclonal antibody (I-19; Santa Cruz), were determined a loading control.

Microarray analysis

Wild type, $Trp53^{stop5/-}$ and $Trp53^{-/-}$ ES cells were cultured as a monoculture for 26 hours (using a 0.1% gelatin coating, no feeder layers were used to prevent mixed cell type sampling). Proliferation rates of all the four genotypes (including the *p53.E5stop.M41I* variant) were in the same range and were examined by XTT test (Roche) (results not shown). Total RNA was isolated using the RNeasy Mini Kit (Qiagen, Valencia, CA, USA). RNA quality was tested using automated gel electrophoresis (Bioanalyzer 2100; Agilent technologies, Amstelveen, the Netherlands). All RNA samples used had an RNA integrity number (RIN) > 9.9.

RNA samples (Wild type $Trp53^{+/+}$, $Trp53^{stop5/-}$, $Trp53^{-/-}$: n = 5 per genotype) were labeled and hybridized to Mouse GeneChip 430 2.0 (Affymetrix, Santa Clara, CA, USA) according to manufacturer's protocol. Due to technical quality control one $Trp53^{-/-}$ sample was discarded as a technical outlier.

The microarray data were normalized by RMA [38] using a custom CDF as described by de Leeuw et al [39]. Of the hybrid probe set definitions included in the annotation, 16.331 probe sets (http://brainarray.mbni.med.umich.edu/Brainarray/Database/CustomCDF) and the 4.648 Affymetrix probe sets corresponding to an Entrez Gene ID were used in further analysis. Subsequent data analyses were performed using R [40], Microsoft Excel and GeneMaths (Sint-Martens-Latem, Belgium). Log transformed gene expression values were compared between a pair of two groups using a Welch's T-test, and genes with a p-value <0.001 and a fold ratio (defined as maximum/minimum average group value) > 1.5 were considered differentially expressed. Functional annotation and Gene Ontology term enrichment was performed using the DAVID/EASE [41;42] web application. The normalized enrichment

score (NES) reflects the degree of overrepresentation of a gene set at the top or bottom of a ranked list of genes, which is then normalized to account for the size of the set and underlying correlations. Q-PCR analysis on *Trp53* (Mm01731290_g1, Applied Biosystems) was performed to check and verify *Trp53* gene expression in the different genotypes.

Results

P53 mutational analysis in urinary bladder tumors

In our previous study [16], wild type, *Trp53*$^{+/-}$ and *Xpa*$^{-/-}$*/Trp53*$^{+/-}$ mice were exposed to either 2-AAF or control feed. Of the 49 2-AAF exposed wild type mice there was only 1 mouse with a urinary bladder tumor, in contrast to the other two genotypes. Of the *Trp53*$^{+/-}$ and *Xpa*$^{-/-}$*/Trp53*$^{+/-}$ mice 29% (12 out of 45) and 63% (22 out of 40) carried urinary bladder tumors. To analyze the integrity of the p53 protein in urinary bladder tumors induced by 2-AAF-exposure, we stained tumor samples of the *Trp53*$^{+/-}$ and *Xpa*$^{-/-}$*/Trp53*$^{+/-}$ mice with the CM5 antibody and the Pab240 antibody (data not shown) to identify positive mutant p53 tumor fields. Sequence analysis of exon 2 to 8 was carried out on DNA isolated from both mutant p53 positive and negative tumor fields. The DNA sequence results are summarized in Table 1 and mutational hotspots are depicted in Figure 1.

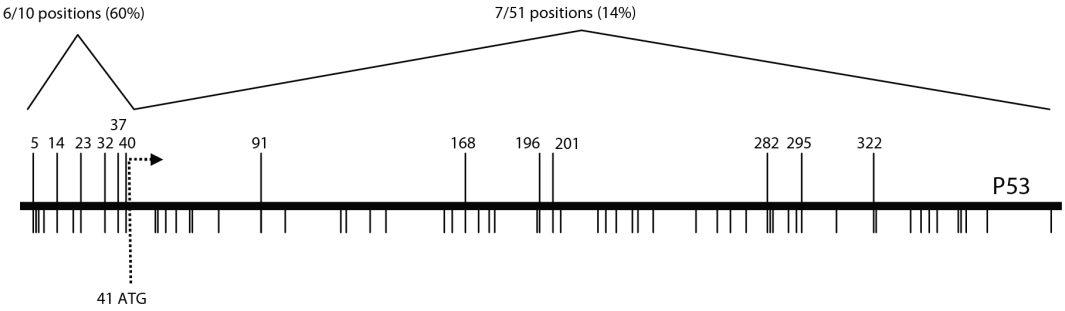

Figure 1. Mutational target sites for nonsense mutations in p53 in 2-AAF exposed urinary bladder tumors. Possible mutational transversion G:C → T:A targets in the p53 protein that can transverse into a stop codon due to a 2-AAF driven G:C → T:A transversion are indicated by bars below the schematic p53 protein. Numbered targets depicted above the schematic p53 protein were discovered in urinary bladder tumors after exposure to 2-AAF. Location 41 indicates an alternative start site in p53, upstream of codon 41.

In total, 78% of the examined urinary bladder tumors (21 out of 27) harbored a mutation in the *Trp53* gene. A wide variety of *Trp53* mutations was observed (Table 1). The majority of mutations identified were single base changes found in *Trp53* DNA. Mutations were confirmed at the mRNA level, indicating that p53 transcripts were stable even though many of them carried a translational stop codon at the 5' region of the transcript. The mutations comprised predominantly G:C → T:A transversions (28 out of 36 single base mutations = 78%), consistent with the mutations frequently found after 2-AAF exposure [17;18]. In compliance with previous exposure studies, 61% of the mutations were found in the DNA binding domain (exon 4 to 8) were missense mutations (14 from 23).

Codon	Exon	Base change*	Amino acid change**	Frequency affected***	Genotype
5	**2**	**GAG→TAG**	**Glu→Stop**	**1**	*Trp53*$^{+/-}$
14	**2**	**GAG→TAG**	**Glu→Stop**	**4**	*Trp53*$^{+/-}$ + *Xpa*$^{-/-}$/*Trp53*$^{+/-}$
23	**2**	**TCA→TAA**	**Ser→Stop**	**3**	*Trp53*$^{+/-}$ + *Xpa*$^{-/-}$/*Trp53*$^{+/-}$
32	**3**	**GAA→TAA**	**Glu→Stop**	**1**	*Trp53*$^{+/-}$
	3-4	del	del 36-122	2	*Xpa*$^{-/-}$/*Trp53*$^{+/-}$
37	**4**	**TCA→TAA**	**Ser→Stop**	**1**	*Trp53*$^{+/-}$
40	**4**	**TGC→TGA**	**Cys→Stop**	**1**	*Xpa*$^{-/-}$/*Trp53*$^{+/-}$
91	**4**	**TCA→TAA**	**Ser→Stop**	**1**	*Trp53*$^{+/-}$
114	4	GGG→GAG	Gly→Glu	1	*Xpa*$^{-/-}$/*Trp53*$^{+/-}$
122	4	ACG→AAG	Thr→Lys	1	*Xpa*$^{-/-}$/*Trp53*$^{+/-}$
124	5	TCT→TTT	Ser→Phe	1	*Xpa*$^{-/-}$/*Trp53*$^{+/-}$
131	5	TTC→TTA	Phe→Leu	1	*Trp53*$^{+/-}$
168	**5**	**GAG→TAG**	**Glu→Stop**	**1**	*Xpa*$^{-/-}$/*Trp53*$^{+/-}$
176	5	CAT→AAT	His→Asn	1	*Trp53*$^{+/-}$
176	5	CAT→TAT	His→Tyr	1	*Xpa*$^{-/-}$/*Trp53*$^{+/-}$
	Intron 5/exon 6	agGC-atGC		1	*Xpa*$^{-/-}$/*Trp53*$^{+/-}$
196	**6**	**GGA→TGA**	**Gly→Stop**	**1**	*Trp53*$^{+/-}$
201	**6**	**GAG→TAG**	**Glu→Stop**	**1**	*Trp53*$^{+/-}$
202	6	TAT→TTT	Tyr→Phe	2	*Trp53*$^{+/-}$
	Intron 7/exon 8	agTG→atTG		1	*Xpa*$^{-/-}$/*Trp53*$^{+/-}$
	Intron 7/exon 8	agTG-aaTG		1	*Xpa*$^{-/-}$/*Trp53*$^{+/-}$
238	7	TCC→TAC	Ser→Tyr	1	*Xpa*$^{-/-}$/*Trp53*$^{+/-}$
253	7	ACA→AAA	Thr→Lys	1	*Trp53*$^{+/-}$
270	8	CGT→CTT	Arg→Leu	1	*Xpa*$^{-/-}$/*Trp53*$^{+/-}$
276	8	GGG→AGG	Gly→Arg	1	*Xpa*$^{-/-}$/*Trp53*$^{+/-}$
278	8	GAC→TAC	Asp→Tyr	1	*Xpa*$^{-/-}$/*Trp53*$^{+/-}$
282	**8**	**GAA→TAA**	**Glu→Stop**	**1**	*Xpa*$^{-/-}$/*Trp53*$^{+/-}$
291	8	GTC→GCC	Val→Ala	1	*Xpa*$^{-/-}$/*Trp53*$^{+/-}$
295	**8**	**GAA→TAA**	**Glu→Stop**	**2**	*Trp53*$^{+/-}$ + *Xpa*$^{-/-}$/*Trp53*$^{+/-}$
322	**9**	**GGA→TGA**	**Gly→Stop**	**1**	*Trp53*$^{+/-}$

Table 1. Analysis of *Trp53* mutations in 2-AAF induced urinary bladder tumors of *Trp53*$^{+/-}$ and *Xpa*$^{-/-}$/*Trp53*$^{+/-}$ mice by direct sequencing. * The affected nucleotide is underlined. ** Nonsense mutations are indicated in bold. *** Indicates in how many different tumors from different animals the mutation has been found.

Of the single base mutations, 53% (19 out of 36) were nonsense mutations. Of these, a relatively high percentage (11 out of 19 = 63%) was found between codon 1 and 41 of the N-terminal part of the p53 protein. To illustrate this bias: 6 of the 10 (60%) possible G:C → T:A transversion target sites (amino acids that can be changed into a nonsense codon by a G:C→T:A transversion) upstream of codon 41, which may lead to a nonsense codon, were found mutated in the tumor set analyzed in this study. In

contrast, only 7 out of 51 (14%) in the remaining part of the p53 protein (Table 1 and Figure 1), which is a significant difference (p = 0.0011 Chi-square test). Additionally, some of these nonsense mutations were present more frequently for a few codons (Table 1). These nonsense mutations at the 5' end of the *Trp53* gene accounted for 31% (11 out of 36) of the total number of single base p53 mutations found. Clearly, a selection of nonsense mutations at the extreme 5' end of the *p53* gene seems to occur after 2-AAF exposure.

No p53 protein was detectable by immunohistochemistry in tumors carrying a nonsense mutation present downstream of codon 41 (data not shown). However, when staining was performed on a selection of tumors containing nonsense codons upstream of codon 41 (codons 5, 14 and 23 were investigated) the presence of p53 protein was still observed, as was shown by immunohistochemistry analyses using both CM5 (Figure 2C) and Pab240 antibody (staining not shown). These tumor fields did not however show staining with the 1C12 antibody (Figure 2D), only recognizing the N-terminal part of the p53 protein. Therefore, an altered version of the p53 protein appears to be present lacking some amino acid residues at the N-terminus (Figure 2).

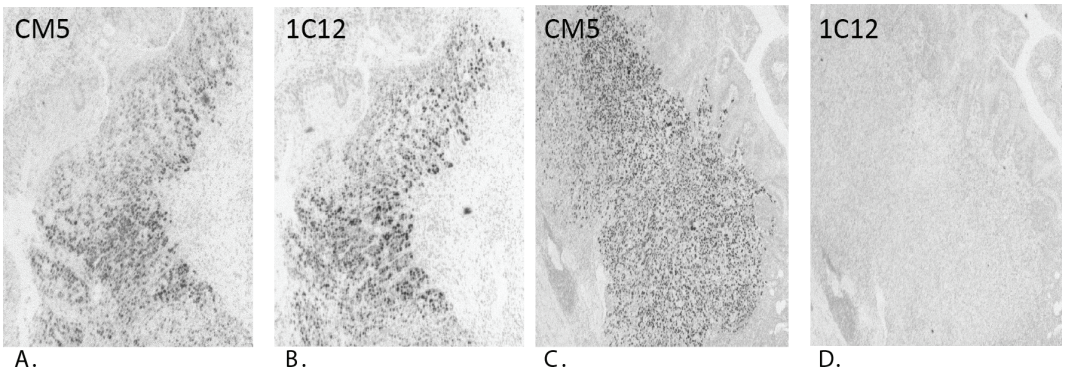

Figure 2. Immunohistochemistry staining of a 2-AAF-induced urinary bladder tumor. **A, C.** CM5 antibody staining in two different urinary bladder tumors. **B, D.** 1C12 antibody staining in two different urinary bladder tumors. The tumor shown in 2A and B carries a mutant p53 protein including the N-terminal part. The tumor shown in 2C and D carries a mutant p53 protein, missing the N-terminal part (1C12 negative).

Functional analysis of nonsense mutations at the 5' end of Trp53 in ES cells

A downstream ATG site in the *Trp53* sequence is present at codon 41, surrounded by sequences that match the Kozak consensus criteria [19]. This codon may, therefore, act as an alternative translational start site, which may explain the exhibited absence of 1C12 antibody staining of mutant P53 protein in tumors carrying specific N-terminal stop codons.

To provide evidence for this hypothesis, we generated 2 different knock-in mutant ES cell lines. The targeting constructs were introduced into a p53 null cell line. In one cell line, we introduced a TAG translational stop at codon 5 (stop5), mimicking the p53 mutation found in the 2-AAF induced bladder tumors (Figure 3A + supplemental figure 1A). In a second cell line, this TAG stop codon was complemented with a mutation at codon 41, where this presumptive alternative translational start codon ATG was replaced by an ATA (Ile encoding) codon (stop5 + ATA41, Figure 3A + supplemental

figure 1B). Expression of p53 protein was analyzed by Western blotting (Figure 3B). The cell line carrying the TAG stop at codon 5 led to the expression of a truncated version of the p53 protein; ΔN-p53 (Figure 3B, lane 4). Possible protein products originating from splice variants of both the wild type and the ΔN-p53 isoform are not visible on the Western Blot, but could theoretically still be present in very low amounts. Additional replacement of the alternative start codon 41 eliminated the translation of ΔN-p53 completely (Figure 3B, lane 5), leading to the conclusion that this variant indeed protein originates from translational initiation at codon ATG41. Western blotting (Figure 3B) and Q-PCR analysis of *Trp53* (data not shown) on these two knock-in mutant genotypes showed that the ΔN-p53 variant isoform originates from a stable transcript. Transcripts from the double mutant (stop5 + ATA41) however appeared to be unstable, only 4% steady state levels, as compared to wild type, were observed. This again supports our view that the ATG41 is used as a start signal for translation, which leads to stabilization of the transcript.

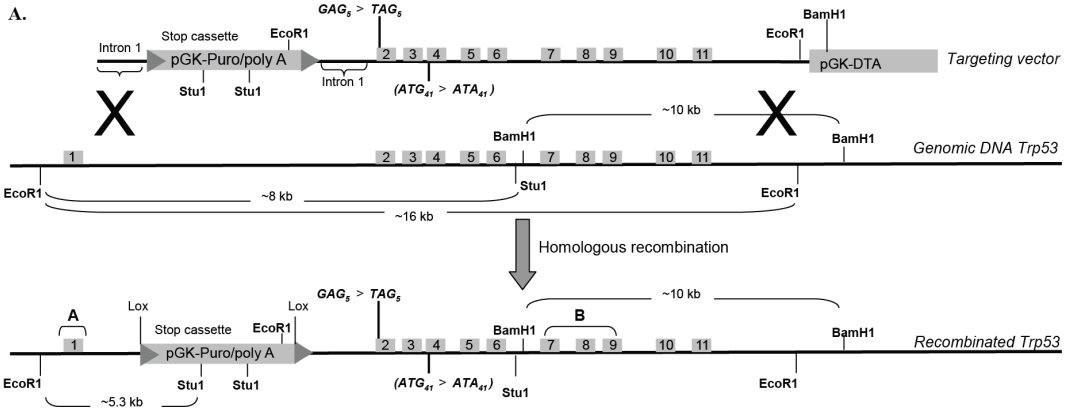

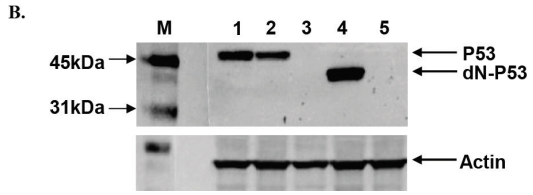

Figure 3. **A.** Schematic representation of the targeting construct (stop5) and (stop5 + ATA41) used for introducing a stop codon at codon 5 (and an isoleucine at the alternative startcodon at codon 41) in the p53 gene. The stop cassette contains a selective puromycin marker flanked by LoxP sites and a pGK-DTA selection marker is introduced at the 3' end of the construct. **B.** Western blot analysis of p53 and ΔN-p53 in control and knocked in ES cells. Lane 1. *Trp53*$^{+/+}$ Lane 2. *Trp53*$^{+/-}$ Lane 3. *Trp53*$^{-/-}$ Lane 4. *Trp53*$^{stop5/-}$ Lane 5. *Trp53*$^{stop5\ +\ ATA41/-}$.

Transcriptomics in ES cells carrying the ΔN-p53 protein

Subsequently, gene expression profiles of ES cells with various genotypes were analyzed to examine the functional impact of the p53 isoform and to investigate whether it showed differences with a p53 knock-out genotype. The genotypes studied included wild type (*Trp53*$^{+/+}$), knock-out p53 (*Trp53*$^{-/-}$) and cells that harbored a stop mutation at codon 5 in one allele combined with a deletion of the other p53 allele (*Trp53*$^{stop5/-}$).

When *Trp53*$^{-/-}$ and *Trp53*$^{stop5/-}$ ES cells are compared to wild type cells these genotypes both show a divergent regulated expression from the wild type cells (Figure 4A). Although *Trp53*$^{stop5/-}$ ES cells show quite some overlap in gene expression with the p53 knock out ES cells (Cat.2, 348 genes), there were differences apparent between the two genotypes. In general, more genes appear transcriptionally regulated (p< 0.001 and Fold Ratio (FR) > 1.5) in *Trp53*$^{stop5/-}$ (838 genes) compared to *Trp53*$^{-/-}$ (567 genes). Additionally, 490 genes (Cat.3) are significantly regulated in *Trp53*$^{stop5/-}$ ES cells only, which is more than double the amount of significantly regulated genes in the knock-out ES cells only (Cat.1, 219 genes).

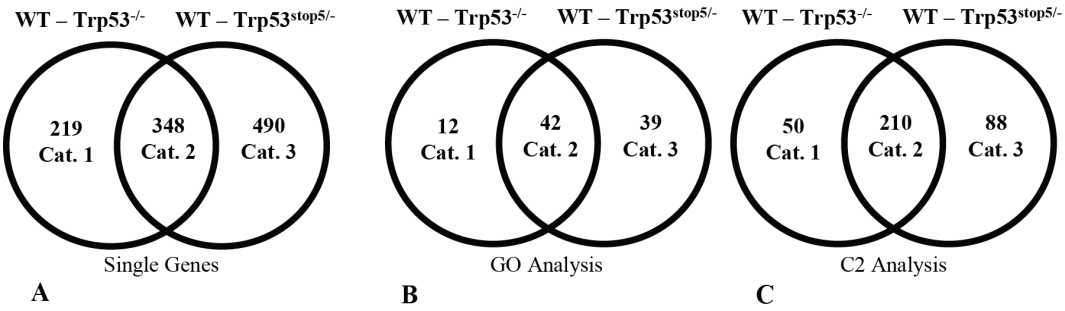

Figure 4. Venn diagram (p<0.001 and FR> 1.5) of differential gene-expression (**A**) and gene ontology (GO) (**B**) and gene set enrichment (C2) (**C**) analysis between wild type versus *Trp53*$^{-/-}$ and wild type versus *Trp53*$^{stop5/-}$ genotypes. Category 1 indicates the number of parameters (single genes, GO or C2) solely significantly regulated between wild type and *Trp53*$^{-/-}$ cells. Category 3 indicates the number of parameters (single genes, GO or C2) solely significantly regulated between wild type and *Trp53*$^{stop5/-}$ cells. Category 2 shows the overlapping parameters between both the genotype comparisons. Categories 1 + 2 together indicate the total number of significantly regulated parameters (single genes, GO or C2) between wild type and *Trp53*$^{-/-}$ cells. Categories 2 + 3 together indicate the total number of significantly regulated parameters between wild type versus *Trp53*$^{stop5/-}$ genotypes.

Whole genome analyses on gene ontology (GO) and gene set enrichment (C2) (p<0.005 and FDR = 0.1) on wild type versus *Trp53*$^{-/-}$ and wild type versus *Trp53*$^{stop5/-}$ genotypes was performed (Figure 4B + 4C). Again, *Trp53*$^{stop5/-}$ appears to be more differentially (de)regulated compared to wild type than *Trp53*$^{-/-}$, but both show a larger overlap (42 GO terms and 210 gene sets overlap, Cat. 2 in Figure 4B + 4C) when compared to the transcriptionally significant regulated single genes in Figure 4A. These results together indicate that the present ΔN-p53 isoform does in some way reacts similar to the knock-out genotype, but also shows aberrant regulation in several pathways and gene sets. 39 GO terms (Cat.3, Figure 4B) seem to be divergently regulated only in *Trp53*$^{stop5/-}$ when compared to wild type, and not when the knock-out is compared to wild type. Amongst these are several developmental processes, plus the GO terms extracellular space, angiogenesis and actin filament binding. C2 analysis resulted in 88 gene sets (Cat.3, Figure 4C) which are only significantly regulated in the *Trp53*$^{stop5/-}$

compared to wild type cells. A full overview of the GO and C2 analyses is shown in the Supplementary Info Table 1 (data not shown in this thesis).

A

GO pathway	NES
Extracellular Matrix*	2,08
Collagen*	2,07
Proteinaceous Extracellular Matrix*	2,06
Structural Constituent of Muscle	2,03
Extracellular Matrix Part*	1,98
Regulation of Heart Contraction	1,92
Muscle Development	1,88
Actin Cytoskeleton*	1,87
Developmental Maturation*	1,86
Structural Molecule Activity*	1,83

B

C2 gene set	Description gene set	NES
VEGF_MMMEC_6HRS_UP*	Up-regulated at 6hrs following VEGF treatment of human myometrial microvascular endothelial cells	2,17
CROONQUIST_IL6_STROMA_UP*	Genes upregulated in multiple myeloma cells exposed to the pro-proliferative cytokine IL-6 versus those co-cultured with bone marrow stromal cells	2,14
IRITANI_ADPROX_VASC*	Blood vascular EC	2,13
GILDEA_BLADDER_UP*	Top 30 genes differentially expressed in metastatic (T24T) and nonmetastatic (T24) human bladder cancer cell lines	2,03
VEGF_MMMEC_12HRS_UP	Up-regulated at 12hrs follwing VEGF treatment of human myometrial microvascular endothelial cells	2,03
HSA04510_FOCAL_ADHESION*	Focal adhesion	2,02
TSA_HEPATOMA_CANCER_UP*	Cancer-related genes up-regulated in any of four human hepatoma cell lines following 24-hour treatment with 200ng/mL of trichostatin A	2,02
HSA01430_CELL_COMMUNICATION*	Genes involved in cell communication	1,99
CORDERO_KRAS_KD_VS_CONTROL_UP*	Genes up-regulated in kras knockdown vs control in a human cell line	1,98
BRENTANI_CELL_ADHESION	Cancer related genes involved in cell adhesion and metalloproteinases	1,95
JECHLINGER_EMT_UP	Genes up-regulated for epithelial plasticity in tumor progression	1,93
IGLESIAS_E2FMINUS_UP*	Genes that increase in the absence of E2F1 and E2F2	1,93
HSA04512_ECM_RECEPTOR_INTERACTION*	Genes involved in ECM-receptor interaction	1,92
EMT_UP*	Up-regulated during the TGFbeta-induced epithelial-to-mesenchymal transition (EMT) of Ras-transformed mouse mammary epithelial (EpH4) cells (EMT is representative of late-stage tumor progression and metastasis)	1,89
LEE_MYC_E2F1_UP*	Genes up-regulated in hepatoma tissue of Myc+E2f1 transgenic mice	1,88
TGFBETA_ALL_UP*	Up-regulated by TGF-beta treatment of skin fibroblasts, at any time point	1,87
TGFBETA_EARLY_UP*	Up-regulated by TGF-beta treatment of skin fibroblasts at 30 min (clusters 1-3)	1,85
TGFBETA_C2_UP	Up-regulated by TGF-beta treatment of skin fibroblasts, cluster 2	1,83
LEE_E2F1_UP*	Genes up-regulated in hepatoma tissue of E2f1 transgenic mice	1,81
RUTELLA_HEPATGFSNDCS_UP	Genes up-regulated by HGF treatments, growth factor treatment	1,79
BRCA_BRCA1_NEG*	Genes whose expression is consistently negatively correlated with brca1 germline status in breast cancer - higher expression is associated with BRCA1 tumors	1,75
BAF57_BT549_UP*	Up-regulated following stable re-expression of BAF57 in Bt549 breast cancer cells that lack functional BAF57	1,75
BRCA1_OVEREXP_PROSTATE_UP*	Up-regulated with stable, ectopic overexpression of BRCA1 in DU-145 human prostate cancer cell lines, compared to neo-only controls	1,69
HDACI_COLON_BUT12HRS_UP*	Up-regulated by butyrate at 12 hrs in SW260 colon carcinoma cells	1,67

Table 2. Significant differential Gene Ontology pathways (**A**) and GSEA C2 gene sets (**B**) between *Trp53*$^{stop5/-}$ and *Trp53*$^{-/-}$ genotypes. p<0.005 and FDR = 0.1, NES = normalized enrichment score. * Already significantly differential from wild type in *Trp53*$^{-/-}$ and *Trp53*$^{stop5/-}$.

We subsequently conducted whole genome GO and C2 analyses (p<0.005 and FDR = 0.1) between the *Trp53*$^{-/-}$ and the *Trp53*$^{stop5/-}$ genotypes to further elucidate the differences between the two (Supplementary Info Table 2, data not shown in this thesis). The GO analysis shows 10 pathways differentially and significantly regulated between the two genotypes (Table 2A), while 82 gene sets are aberrantly regulated. Seven out of the 10 GO terms overlap with those shown in Figure 4B, and are, therefore, even stronger significantly upregulated in *Trp53*$^{stop5/-}$. Again, collagen and extracellular matrix pathways are more regulated in *Trp53*$^{stop5/-}$ when compared to the knock out ES cells.

The 82 differential C2 gene sets contain several gene sets which are linked to cancer, growth, invasiveness and TGF-beta signaling pathways. Of these gene sets, 48 were present in the overlapping 210 gene sets in Figure 4C, which means they were already significantly differential from wild type in both p53 impaired ES cells. A selection of gene sets is shown in Table 2B. In addition, Supplemental Info Table 3 (data not shown in this thesis) shows a selection of single genes, most of which are involved in the pathways and gene sets mentioned in Table 2.

Discussion

P53 is the most commonly mutated gene in mammalian tumors [20]. Its role as a tumor suppressor in the prevention of cancer is multifaceted, since the p53 protein interacts with and transactivates a wide variety of key proteins. P53-deficient organisms show a strong increase in the rate of tumor onset and subsequently in the development of multiple tumor types [21-23].

In our present study, 2-AAF induced urinary bladder tumors in *Trp53*$^{+/-}$ and *Xpa*$^{-/-}$*/Trp53*$^{+/-}$ mice harboring *Trp53* mutations. Single base mutations, predominantly in specific G:C → T:A transversions, were found. In agreement with other studies [24;25], we found several missense mutations in the DNA binding domain. Interestingly however, a high percentage of nonsense mutations was present predominantly at the 5´ end of the *Trp53* gene. There is a significant selection (p = 0.0011 Chi-square test) for these N-terminal nonsense mutations found in the bladder tumors induced after 2-AAF exposure.

Immunohistochemical staining confirmed that p53 protein was present in the tumor cells, but the protein lacked the N-terminal domain. Using homologous recombination experiments in ES cells we demonstrated that codon 41 is used as a novel start site when a nonsense mutation is present at codon 5. This is most likely also the case for the other nonsense mutation variants we found located upstream of codon 41 (Table 1). The manner in which this 'forced' isoform translation takes place due to the 5' nonsense mutations is unknown and needs further investigation. Previous reports have shown that internal ribosomal entry sites (IRES) can play a role and can be phase-dependent on the cell cycle [4;26]. Another option might be that translational leakage occurs and 'false' initiation takes place at codon 41, which is surrounded by a Kozak consensus sequence [19].

The existence of ΔN-p53 has already been reported [1;27], but up to now it was not known that selectively induced N-terminal stop mutations could be the origin of this p53-isoform. Unlike many other studies which have only focused on sequencing the DNA binding domain (exon 4 to 8) our studies characterized exon 2 to 8 of the *Trp53* gene. This could be one of the reasons why these

specific 5' end stop mutations went undetected until now. Additionally, bladder tumors are not amongst the most commonly found tumor types.

Previously, it was shown that ΔN-p53 originates from alternative splicing events [28;29] or occurs as a natural isoform [1;30]. Courtois et al. proposed that alternative translation initiation at codon 41 was not inducible in response to stress [1]. However, our results show that genotoxic stress can be a cause of selection for the ΔN-p53 isoform due to the 2-AAF induced 5' end nonsense mutations.

It has been reported that ΔN-p53 does not carry autonomous transcriptional activity, most likely due to the lack of the N-terminal transactivation domain [1;3;29]. However, Powell et al. performed vector transfection induced expression in H1299 human lung cells, conducted macroarray profiling investigating 84 p53-related genes and showed stress-dependent changes in gene expression [31]. Ohki et al. showed deletion of the complete p53 first activation domain (including the alternative start codon 41) in *Saos2*-cells induced apoptotic genes that were not induced by the full length p53 [32]. We are the first to investigate if the ΔN-p53 isoform has different functional transcriptional properties in a stable knock-in mutant cell line, comparing untreated cells to wild type and p53 knock out cell lines derived from the same genetic background on a full genome scale.

Results showed a clear difference at the transcriptional level between the wild type and both the the *Trp53*$^{stop5/-}$ and *Trp53*$^{-/-}$ ES cells, but additional evident disparities between the *Trp53*$^{stop5/-}$ and *Trp53*$^{-/-}$ genotypes were also discovered. Several developmental and regulatory processes, together with pathways involved in extracellular space, angiogenesis and actin filament binding are expressed at higher levels in *Trp53*$^{stop5/-}$ cells than in p53 knock out cells. The same holds when GO term analysis was applied, processes involved in the formation of the extracellular matrix and the production of collagen are expressed at higher levels in *Trp53*$^{stop5/-}$ cells than *Trp53*$^{-/-}$ cells (Table 2A). These pathways are also found upregulated in invasive tumors and are known to be involved in metastasis [33;34]. Additionally, gene sets (Table 2B) and single genes (Supplemental Info Table 3) which are correlated with cancer, growth, invasiveness, metastasis and TGF-beta signaling are significantly regulated in an increased manner in *Trp53*$^{stop5/-}$ ES cells when compared to knock-out cells.

The effects on gene expression were all examined in ES cells and suggest that *Trp53*$^{stop5/-}$ cells have a distinct phenotype compared to *Trp53*$^{-/-}$ cells. However, the selective outcome of exposure to 2-AAF was seen in epithelial bladder tissue. For a fair characterization of the functional effect of ΔN-p53 an *in vivo* analysis is more suitable. We, therefore, are currently creating mouse models which transcribe the isoform of p53 in different genotypical backgrounds (*Trp53*$^{stop5/+}$ and *Trp53*$^{stop5/-}$). Exposure of these models to 2-AAF and/or other stressors should shed more light on the origin, selection and function of the p53 isoform. Additionally, it can not be excluded that the gene expression profiles of wild type and *Trp53*$^{stop5/-}$ cells are also influenced by splice variants of *Trp53*. Some splice variants of *Trp53* which are present in normal cells might also occur for the ΔN-p53 isoform, therefore the expression profiles could be the result of a combined expression, eventhough Western blotting shows no additional other sized proteins.

In conclusion, our data suggest that the N-terminal truncated p53 isoform can originate upon genotoxic stress due to the introduction of selective nonsense mutations in the p53 gene. Additionally, this study provides evidence that the transcriptional activity in cells expressing the ΔN-p53 isoform is

functionally divergent from p53 knock-out cells and may lead to an even more malignant phenotype and possibly has some gain-of-function properties.

Conflict of interest

The authors declare no conflict of interest.

Acknowledgements

We would like to thank the Animal Facilities of the Netherlands Vaccine Institute (NVI) for their skillful (bio)technical support. The work presented here was in part supported by NIH/NIEHS (Comparative Mouse Genomics Centers Consortium) grant 1UO1 ES11044.

Supplementary information is available at www.nature.com/onc/index.html

Reference List

[1] S.Courtois, G.Verhaegh, S.North, M.G.Luciani, P.Lassus, U.Hibner, M.Oren, P.Hainaut. DeltaN-p53, a natural isoform of p53 lacking the first transactivation domain, counteracts growth suppression by wild-type p53, Oncogene, 21, (2002) 6722-6728.

[2] M.M.Candeias, D.J.Powell, E.Roubalova, S.Apcher, K.Bourougaa, B.Vojtesek, H.Bruzzoni-Giovanelli, R.Fahraeus. Expression of p53 and p53/47 are controlled by alternative mechanisms of messenger RNA translation initiation, Oncogene, 25, (2006) 6936-6947.

[3] V.Marcel, P.Hainaut. p53 isoforms - a conspiracy to kidnap p53 tumor suppressor activity?, Cell Mol.Life Sci., 66, (2009) 391-406.

[4] R.Grover, M.M.Candeias, R.Fahraeus, S.Das. p53 and little brother p53/47: linking IRES activities with protein functions, Oncogene, (2009).

[5] C.Heinlein, F.Krepulat, J.Lohler, D.Speidel, W.Deppert, G.V.Tolstonog. Mutant p53(R270H) gain of function phenotype in a mouse model for oncogene-induced mammary carcinogenesis, Int.J.Cancer, 122, (2008) 1701-1709.

[6] S.W.Wijnhoven, E.Zwart, E.N.Speksnijder, R.B.Beems, K.P.Olive, D.A.Tuveson, J.Jonkers, M.M.Schaap, B.J.van den, T.Jacks, H.van Steeg, A.de Vries. Mice expressing a mammary gland-specific R270H mutation in the p53 tumor suppressor gene mimic human breast cancer development, Cancer Res., 65, (2005) 8166-8173.

[7] E.M.Hoogervorst, W.Bruins, E.Zwart, C.T.van Oostrom, G.J.van den Aardweg, R.B.Beems, B.J.van den, T.Jacks, H.van Steeg, A.de Vries. Lack of p53 Ser389 phosphorylation predisposes mice to develop 2-acetylaminofluorene-induced bladder tumors but not ionizing radiation-induced lymphomas, Cancer Res., 65, (2005) 3610-3616.

[8] A.de Vries, E.R.Flores, B.Miranda, H.M.Hsieh, C.T.van Oostrom, J.Sage, T.Jacks. Targeted point mutations of p53 lead to dominant-negative inhibition of wild-type p53 function, Proc.Natl.Acad.Sci.U.S.A, 99, (2002) 2948-2953.

[9] T.Iwakuma, G.Lozano. Crippling p53 activities via knock-in mutations in mouse models, Oncogene, 26, (2007) 2177-2184.

[10] A.J.Levine. p53, the cellular gatekeeper for growth and division, Cell, 88, (1997) 323-331.

[11] S.Hailfinger, M.Jaworski, P.Marx-Stoelting, I.Wanke, M.Schwarz. Regulation of P53 stability in p53 mutated human and mouse hepatoma cells, Int.J.Cancer, 120, (2007) 1459-1464.

[12] S.Strano, S.Dell'Orso, S.Di Agostino, G.Fontemaggi, A.Sacchi, G.Blandino. Mutant p53: an oncogenic transcription factor, Oncogene, 26, (2007) 2212-2219.

[13] Y.Xu. Induction of genetic instability by gain-of-function p53 cancer mutants, Oncogene, 27, (2008) 3501-3507.

[14] G.Lozano. The oncogenic roles of p53 mutants in mouse models, Curr.Opin.Genet.Dev., 17, (2007) 66-70.

[15] E.M.Hoogervorst, H.van Steeg, A.de Vries. Nucleotide excision repair- and p53-deficient mouse models in cancer research, Mutat.Res., 574, (2005) 3-21.

[16] E.M.Hoogervorst, C.T.van Oostrom, R.B.Beems, J.van Benthem, S.Gielis, J.P.Vermeulen, P.W.Wester, J.G.Vos, A.de Vries, H.van Steeg. p53 heterozygosity results in an increased 2-acetylaminofluorene-induced urinary bladder but not liver tumor response in DNA repair-deficient Xpa mice, Cancer Res., 64, (2004) 5118-5126.

[17] J.A.Ross, S.A.Leavitt. Induction of mutations by 2-acetylaminofluorene in lacI transgenic B6C3F1 mouse liver, Mutagenesis, 13, (1998) 173-179.

[18] K.H.Vousden, J.L.Bos, C.J.Marshall, D.H.Phillips. Mutations activating human c-Ha-ras1 protooncogene (HRAS1) induced by chemical carcinogens and depurination, Proc.Natl.Acad.Sci.U.S.A, 83, (1986) 1222-1226.

[19] M.Kozak. Compilation and analysis of sequences upstream from the translational start site in eukaryotic mRNAs, Nucleic Acids Res., 12, (1984) 857-872.

[20] L.Y.Lim, N.Vidnovic, L.W.Ellisen, C.O.Leong. Mutant p53 mediates survival of breast cancer cells, Br.J.Cancer, 101, (2009) 1606-1612.
[21] A.Matheu, A.Maraver, M.Serrano. The Arf/p53 pathway in cancer and aging, Cancer Res., 68, (2008) 6031-6034.
[22] A.J.Levine, J.Momand, C.A.Finlay. The p53 tumour suppressor gene, Nature, 351, (1991) 453-456.
[23] M.Hollstein, D.Sidransky, B.Vogelstein, C.C.Harris. p53 mutations in human cancers, Science, 253, (1991) 49-53.
[24] A.Sigal, V.Rotter. Oncogenic mutations of the p53 tumor suppressor: the demons of the guardian of the genome, Cancer Res., 60, (2000) 6788-6793.
[25] T.Soussi. p53 alterations in human cancer: more questions than answers, Oncogene, 26, (2007) 2145-2156.
[26] P.S.Ray, R.Grover, S.Das. Two internal ribosome entry sites mediate the translation of p53 isoforms, EMBO Rep., 7, (2006) 404-410.
[27] B.Maier, W.Gluba, B.Bernier, T.Turner, K.Mohammad, T.Guise, A.Sutherland, M.Thorner, H.Scrable. Modulation of mammalian life span by the short isoform of p53, Genes Dev., 18, (2004) 306-319.
[28] Y.Yin, C.W.Stephen, M.G.Luciani, R.Fahraeus. p53 Stability and activity is regulated by Mdm2-mediated induction of alternative p53 translation products, Nat.Cell Biol., 4, (2002) 462-467.
[29] A.Ghosh, D.Stewart, G.Matlashewski. Regulation of human p53 activity and cell localization by alternative splicing, Mol.Cell Biol., 24, (2004) 7987-7997.
[30] P.S.Ray, R.Grover, S.Das. Two internal ribosome entry sites mediate the translation of p53 isoforms, EMBO Rep., 7, (2006) 404-410.
[31] D.J.Powell, R.Hrstka, M.Candeias, K.Bourougaa, B.Vojtesek, R.Fahraeus. Stress-dependent changes in the properties of p53 complexes by the alternative translation product p53/47, Cell Cycle, 7, (2008) 950-959.
[32] R.Ohki, T.Kawase, T.Ohta, H.Ichikawa, Y.Taya. Dissecting functional roles of p53 N-terminal transactivation domains by microarray expression analysis, Cancer Sci., 98, (2007) 189-200.
[33] H.Denys, G.Braems, K.Lambein, P.Pauwels, A.Hendrix, A.De Boeck, V.Mathieu, M.Bracke, O.De Wever. The extracellular matrix regulates cancer progression and therapy response: implications for prognosis and treatment, Curr.Pharm.Des, 15, (2009) 1373-1384.
[34] S.M.Pupa, S.Menard, S.Forti, E.Tagliabue. New insights into the role of extracellular matrix during tumor onset and progression, J.Cell Physiol, 192, (2002) 259-267.
[35] K.P.Olive, D.A.Tuveson, Z.C.Ruhe, B.Yin, N.A.Willis, R.T.Bronson, D.Crowley, T.Jacks. Mutant p53 gain of function in two mouse models of Li-Fraumeni syndrome, Cell, 119, (2004) 847-860.
[36] T.Jacks, L.Remington, B.O.Williams, E.M.Schmitt, S.Halachmi, R.T.Bronson, R.A.Weinberg. Tumor spectrum analysis in p53-mutant mice, Curr.Biol., 4, (1994) 1-7.
[37] W.Bruins, E.Zwart, L.D.Attardi, T.Iwakuma, E.M.Hoogervorst, R.B.Beems, B.Miranda, C.T.van Oostrom, B.J.van den, G.J.van den Aardweg, G.Lozano, H.van Steeg, T.Jacks, A.de Vries. Increased sensitivity to UV radiation in mice with a p53 point mutation at Ser389, Mol.Cell Biol., 24, (2004) 8884-8894.
[38] R.A.Irizarry, B.M.Bolstad, F.Collin, L.M.Cope, B.Hobbs, T.P.Speed. Summaries of Affymetrix GeneChip probe level data, Nucleic Acids Res., 31, (2003) e15.
[39] W.C.de Leeuw, H.Rauwerda, M.J.Jonker, T.M.Breit. Salvaging Affymetrix probes after probe-level re-annotation, BMC.Res.Notes, 1, (2008) 66.
[40] R Development Core Team. A language and environment for statistical computing. 2008.
[41] G.Dennis, Jr., B.T.Sherman, D.A.Hosack, J.Yang, W.Gao, H.C.Lane, R.A.Lempicki. DAVID: Database for Annotation, Visualization, and Integrated Discovery, Genome Biol., 4, (2003) 3.
[42] D.A.Hosack, G.Dennis, Jr., B.T.Sherman, H.C.Lane, R.A.Lempicki. Identifying biological themes within lists of genes with EASE, Genome Biol., 4, (2003) R70.